Synchronization in Modular Networks

Pratyush Kollepara (Dept. of Physics, BITS Pilani, Goa)

Under the supervision of :
Prof. Sitabhra Sinha (The IMSc, Chennai)

January 2020

1 Introduction

Synchronization is a very interesting phenomena observed in nature. We see it in lighting up of fireflies, firing of neurons etc. A simple model for synchronization in oscillators was given by Yoshiki Kuramoto. [1]

$$\dot{\theta}_i = \omega_i + \frac{K}{N}\sum_j \sin(\theta_j - \theta_i) \tag{1}$$

Each oscillator has an intrinsic frequency ω_i, and is coupled to all N oscillators through the sinusoidal term. When $\omega_i = \omega$, all the oscillators reach a synchronized state where their phase values are equal. If the frequencies are not the same, the coupling K decides whether synchronization is possible or not. A phase transition is observed when the intrinsic frequencies are sampled from a unimodal distribution, for a given σ of the distribution there exists a K_c, below which synchronization will not occur. For a given K, we can observe a critical σ, beyond which synchronization will not be possible. In the original model the network is fully connected. For other network structures, the factor $1/N$ is changed to $1/d_i$, which is the degree of the node i.
In this report, we explore some aspects of synchronization in modular networks.

2 Description of the system

2.1 Modular Network

Community structure has been observed in social networks. It is observed that there are certain regions in the network which are highly connected, and these regions are connected to other regions by significantly lesser number of edges. These regions are called modules and the network is a modular network. A modularity parameter can be defined : $r = \frac{\rho_o}{\rho_i}$. ρ_o is the inter modular connection probability while ρ_i is the intra modular connection density. [3]

To study the behaviour of statistical physics models on modular networks, we generate random networks with modular structure. With a given size of system (N), number of modules (n_m), average degree (k), and the modularity parameter (r) we can generate such networks.

$$\begin{aligned} k = \rho(N-1) &= \rho_o(n_m - 1)n + \rho_i(n-1) \\ \rho_o = r\rho_i \Rightarrow k &= \rho_i[rn(n_m - 1) + n - 1] \\ C &\equiv rn(n_m - 1) + n - 1 \Rightarrow \\ \rho_i &= k/C \\ \rho_o &= rk/C \end{aligned}$$

Once we have the connection probabilities, we can generate random graphs.

2.2 Ising model

The Ising model from statistical physics has been studied on the modular network and it has been shown that it exhibits three different phases (instead of the conventional two phases). The new phase is the modular ordered phase, where the network as a whole is not magnetized but each individual module is magnetized. This region disappears as the modularity is decreased. [3]
This result prompts us to ask the question how XY model spins would behave on a modular network. Since the there is an analogy between XY spins and the Kuramoto oscillators, one perspective of synchronization in modular networks is given by solving the XY model on a modular network.

2.3 XY model

Unlike the Ising model, here the spins can rotate in a 2D space. We study this system through Monte Carlo simulations. We use the Wolff cluster update [4] to evolve the system from a random state to its equilibrium state. The system is evolved for a certain number of steps until the order parameter fluctuates in a region, after this the order parameter or other relevant quantities are recorded. This is done for multiple networks and initial conditions and the required quantities are averaged over.
The XY Hamiltonian is given by $H = -J\sum_{<ij>}\cos(\theta_i - \theta_j)$. To measure order in the system, an order parameter can be defined : $m = \frac{1}{N}\sum_{j=1}^{N} exp(\iota\theta_j)$. To detect the transition point using the Monte Carlo simulation data we use three different methods :

1. Susceptibility $\chi = \frac{<|m|^2>-<|m|>^2}{kT/J}$. The susceptibility shows a singularity in the thermodynamic limit. For finite size systems, maxima of χ can give us an estimate of critical temperature. However the errors in susceptibility become very high in the critical region and it becomes very hard to find the maxima, moreover the location of maxima is very sensitive to system size.

2. Binder Cumulant $b = 1 - \frac{<|m|^4>}{3<|m|^2>^2}$. This quantity is calculated for different system sizes, and the common intersection point of these curves is the critical point. [2]

3. Histograms. Since the order parameter m is a complex quantity, we can plot the distribution of m in a 2D intensity-histogram. The distribution looks like an annulus whose radius shrinks with increasing temperature and it becomes a two dimensional unimodal distribution. By observing the histograms, we can see at what point the distribution becomes unimodal.

2.4 Kuramoto model

We study the Kuramoto model on modular networks in two ways. First, we add an external white noise term to the equation. It becomes a stochastic differential equation which can be simulated through an Euler-like scheme with a modified random noise term Eqn. 2. The second way is to sample the ω's from a normal distribution. These are the two ways we introduce disorder in the system, we expect that their effects will be similar to the effects of temperature in the XY model. For a zero disorder Kuramoto model the system will eventually go into synchronization, which is analogous to zero temperature in the case of XY model.

$$\dot{\theta}_i = \omega_i + \frac{K}{d_i}\sum_j \sin(\theta_j - \theta_i) + \Gamma\eta(t) \;;\quad \langle\eta(t)\eta(t')\rangle = \delta(t'-t) \tag{2}$$

$$\theta_i(t+dt) = \theta_i(t) + \Big[\frac{K}{d_i}\sum_j \sin(\theta_j - \theta_i)\Big]dt + \Gamma\xi\sqrt{dt} \tag{3}$$

The standard way of detecting the transition in Kuramoto model is by getting the order parameter as a function of K for different system sizes. All the curves would intersect at a common point, this would be the K_c. If K is held constant and the variance of distribution is varied, we will get a σ_c. In our noisy Kuramoto system, the strength of noise Γ is analogous to temperature. Therefore we can calculate susceptibility for it, and we can detect the transition using both susceptibility and order parameter curves.

We also approach this problem from an alternative perspective. Consider a bimodular network, the frequencies inside a module are identical but it can differ across the module. The module is fully coupled internally, and there is a single edge joining the two modules. This is the most extreme case of a modular network, and if we can analytically prove that this system can synchronize then any modular network can synchronize.

3 Results

3.1 XY model

We generate random networks for four different system sizes (Table 1) and average degree $< k >$ = 14. Monte Carlo updates using Wolff algorithm are performed starting from a random state, this is done for $r = 0.001, 0.00178, 0.00316,$
0.00562. We can use the Binder's cumulant here by finding their intersection for different system sizes. Susceptibility can also be used, but since it is prone to finite size effects we will use the Binder's cumulant.

S.No.	N	n	n_m
1	512	32	16
2	1024	32	32
3	1024	64	16
4	2048	64	32

Table 1: System sizes for XY model. N : system size, n_m : number of modules, n : size of module.

For all four r values, we see that the modular transition happens at a lower temperature value than the global one Fig. 1 - 4. This is very counter intuitive, it implies that the modules are not ordered but if we look at the full network, it is ordered. If we use the susceptibility, the anomaly is absent for low r, and we see a modular phase. But with increasing system size, we see that the modular and global critical temperatures approach the same value. To resolve this anomaly, we look at the 2D histograms. In the histograms, we will see the transition happening as the distribution becomes uni-modal.

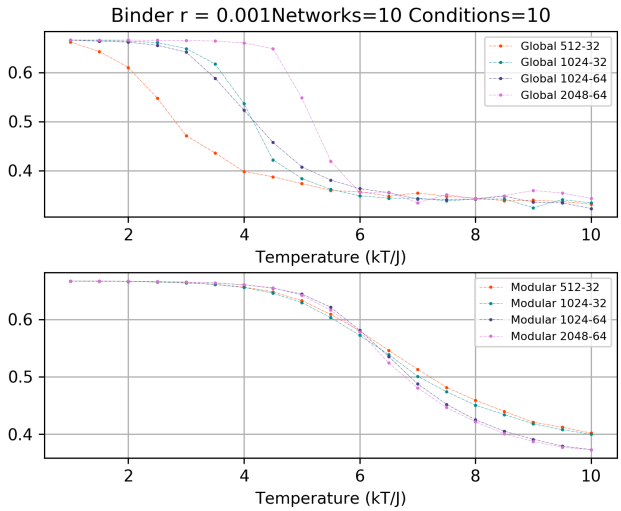

Figure 1: Binder Cumulant, $r = 0.001$. System size are given in the legend $(N - n)$

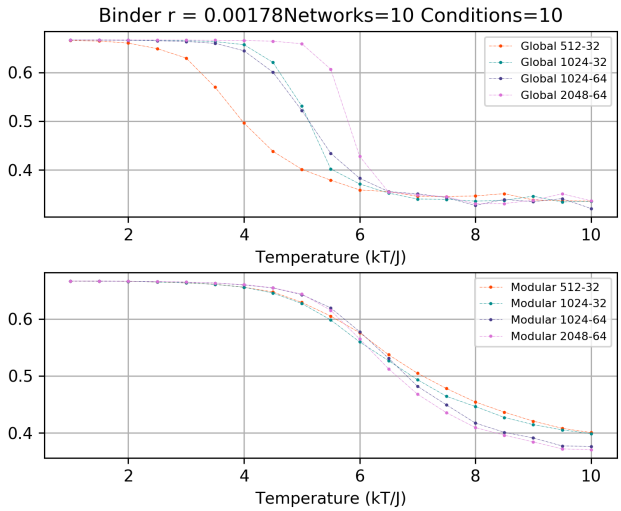

Figure 2: Binder Cumulant, $r = 0.00178$. System size are given in the legend $(N - n)$

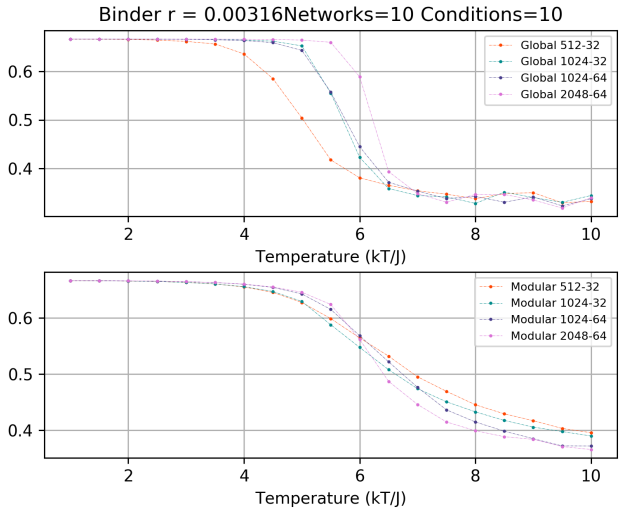

Figure 3: Binder Cumulant, $r = 0.00316$. System size are given in the legend $(N - n)$

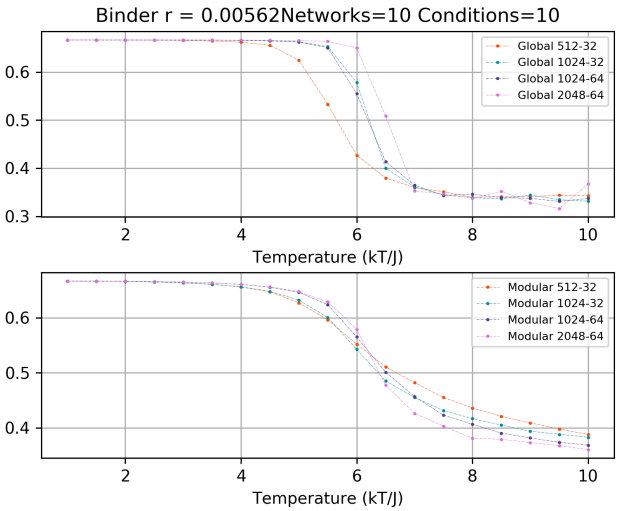

Figure 4: Binder Cumulant, $r = 0.00562$. System size are given in the legend $(N - n)$

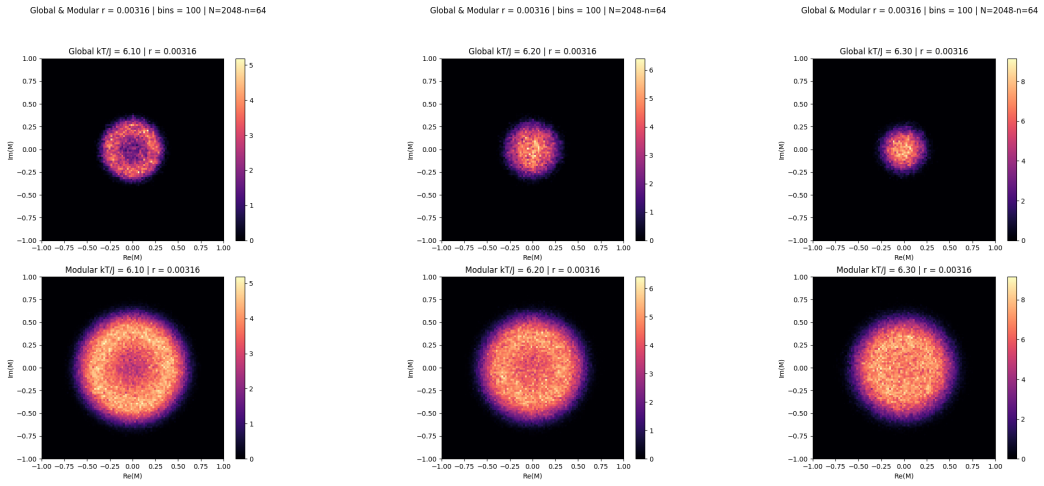

(a) $kT/J = 6.1$ (b) $kT/J = 6.2$ (c) $kT/J = 6.3$

Figure 5: Histogram for r = 0.00316, the global transition happens before the modular transition as expected and suggesting that a modular phase exists.

However, we observe the anomaly here again. For r = 1.0, the modular probability density has become uni-modal before the global one. To resolve this anomaly we have some indication as to why it is happening, we generated 512 random numbers from a Normal distribution with some standard deviation σ and divided into 16 parts, each part representing a module. We can compute the global and modular order parameter for this set. This is done multiple times and 2D histograms can be made. This is further repeated for multiple standard deviations. We would expect that a lower σ would give us an annular distribution and a high σ will lead to a uni-modular distribution. By observing these histograms, we see that the modular transition is indeed happening before the global transition. This leads us to conclude that even in absence of any network structure, we see this kind of anomalous behaviour. Since the global order parameter is computed using the full set, the standard deviation will be small (i.e the width of annulus is small). In the modular case we are averaging over a subset, which leads to a higher standard deviation (i.e a larger width of the annulus). Upon increasing the temperature (or standard deviation of the distribution) the radius of the annulus decreases and it eventually becomes a uni-modal distribution, therefore if the width of the annulus is larger it will become uni-modal before the global one. Even though the anomaly has been explained, we still do not have a proper way of finding the critical point. One method to

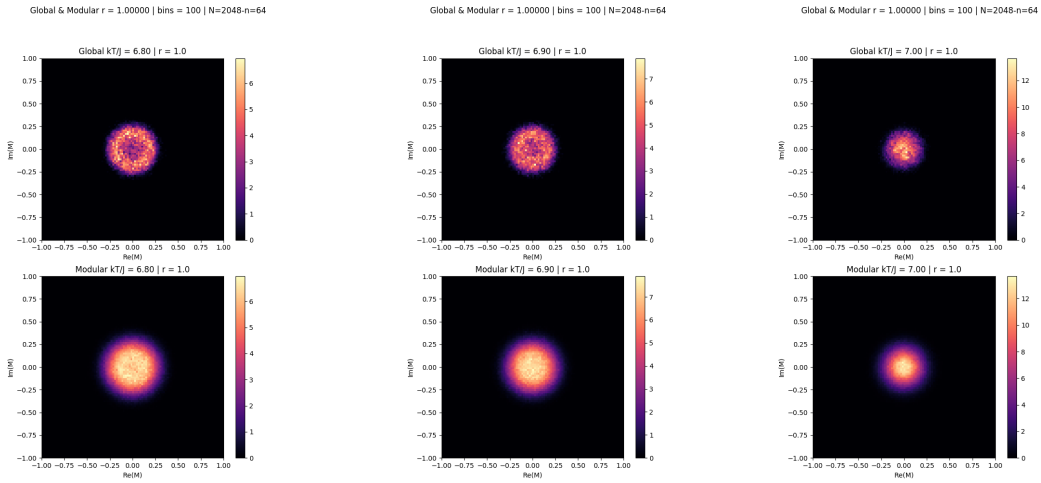

(a) $kT/J = 6.8$ (b) $kT/J = 6.9$ (c) $kT/J = 7.0$

Figure 6: Histogram for r = 1.0, the modular transition happens before the global transition which is very counter intuitive..

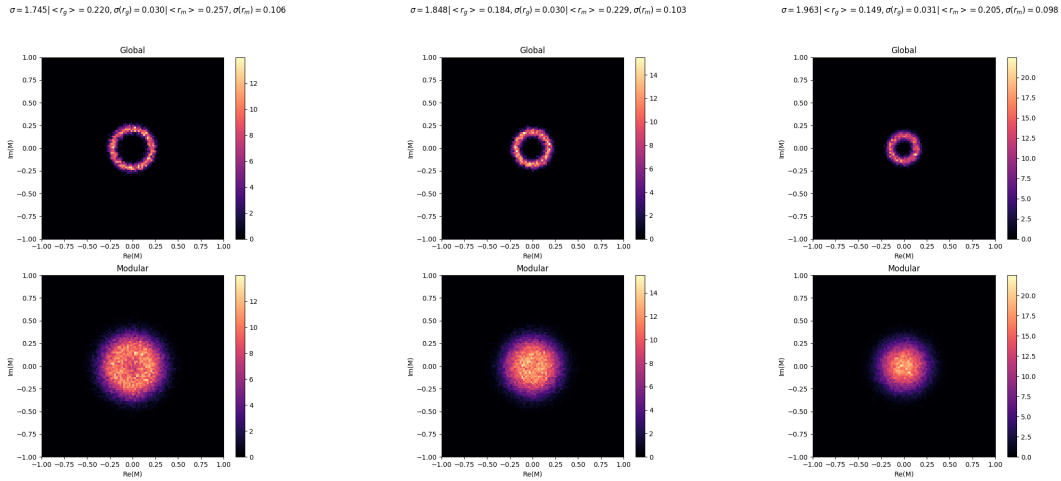

(a) $\sigma = 1.7453$ (b) $\sigma = 1.8480$ (c) $\sigma = 1.9635$

Figure 7: Histogram for randomly generated data.

address this might be to scale the distributions such that they have the same annular width. The phase diagram (constructed using histograms) for $N = 2048, n = 32$ is shown in Fig. 8.

3.2 Kuramoto - Noise

By making an analogy with the XY model, Γ is similar to temperature. And we can use either susceptibility or intersection of magnetization curves to detect the critical noise level. Upon using susceptibility, we see a modular phase for low r values. For higher r we see some anomalies in the transition noise strength. For larger system sizes, we see that the modular phase is less prominent. Fig. 9 - 11.

If we use the intersection of magnetization curves, we observe that the critical noise strength for modular transition is less than the global one. We may conclude that modular order is not possible but the two methods give contrary results, and it is difficult to reach a conclusion. Fig. 12.

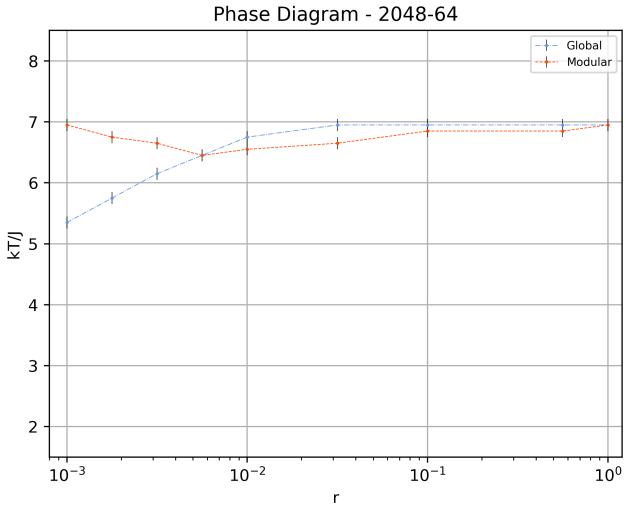

Figure 8: Phase Diagram, $N = 2048, n = 32$. Constructed using histogram, a modular phase exists for small r.

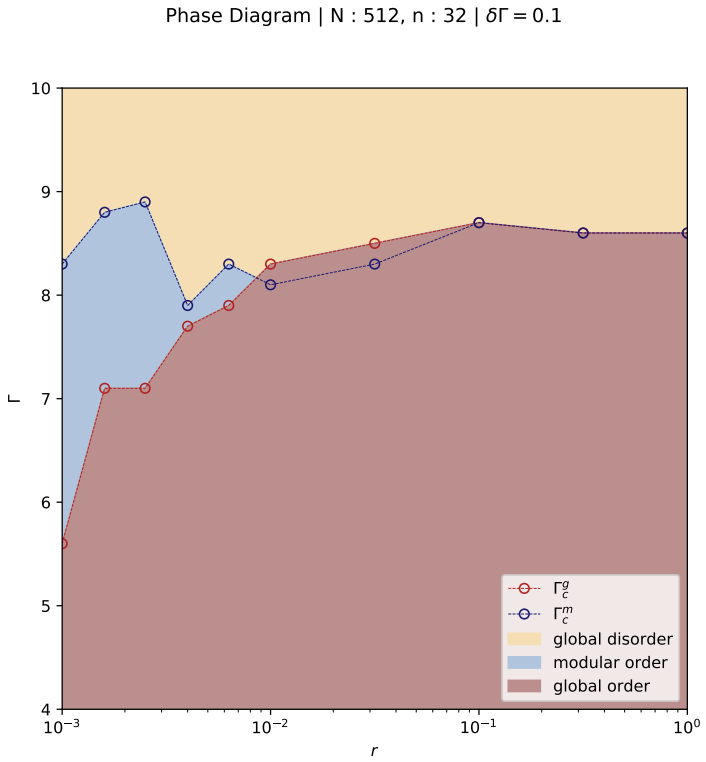

Figure 9: Phase diagram using susceptiblity (Kuramoto with Noise), $N = 512, n = 32$

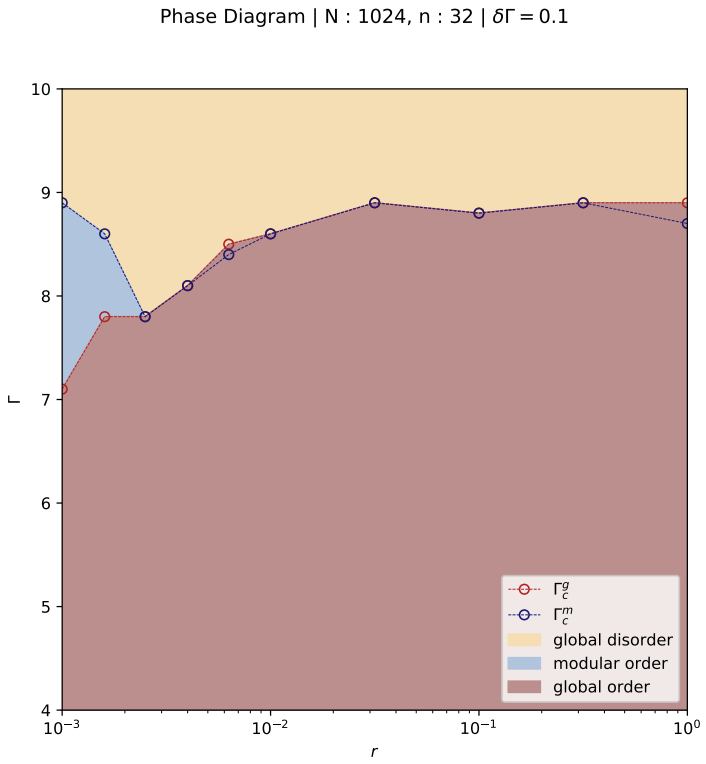

Figure 10: Phase Diagram using susceptiblity (Kuramoto with Noise), $N = 1024, n = 32$

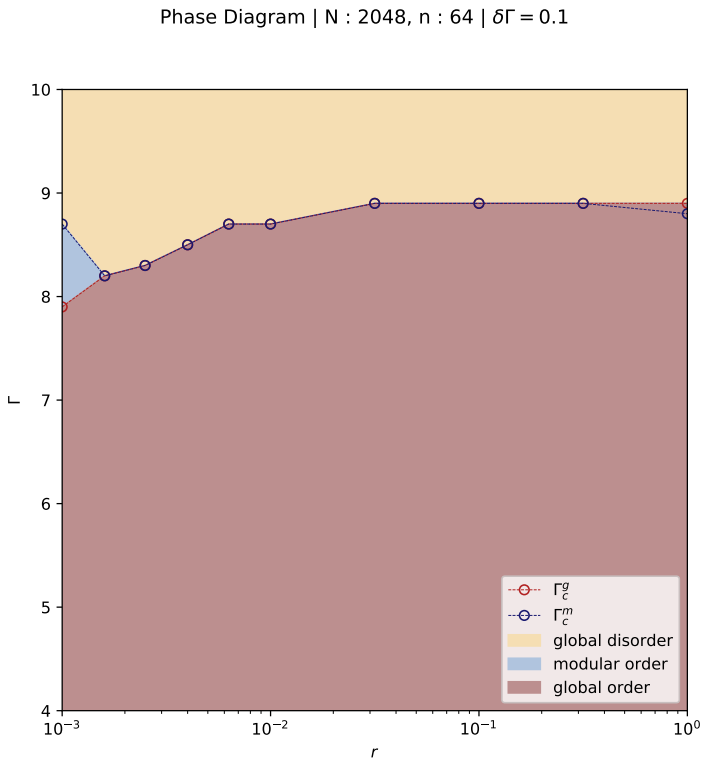

Figure 11: Phase Diagram using susceptiblity (Kuramoto with Noise), $N = 2048, n = 64$

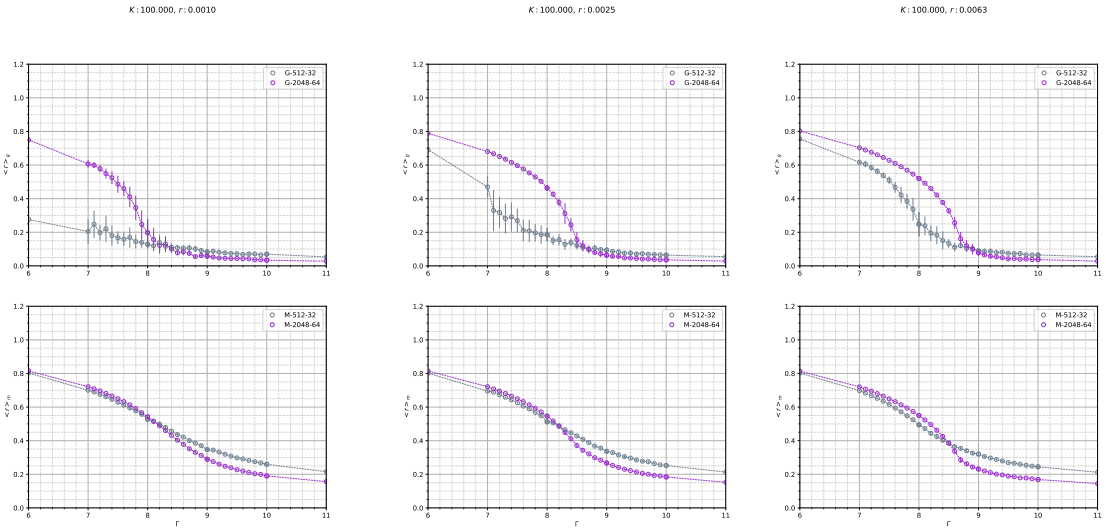

(a) $r = 0.001$ (b) $r = 0.0025$ (c) $r = 0.0063$

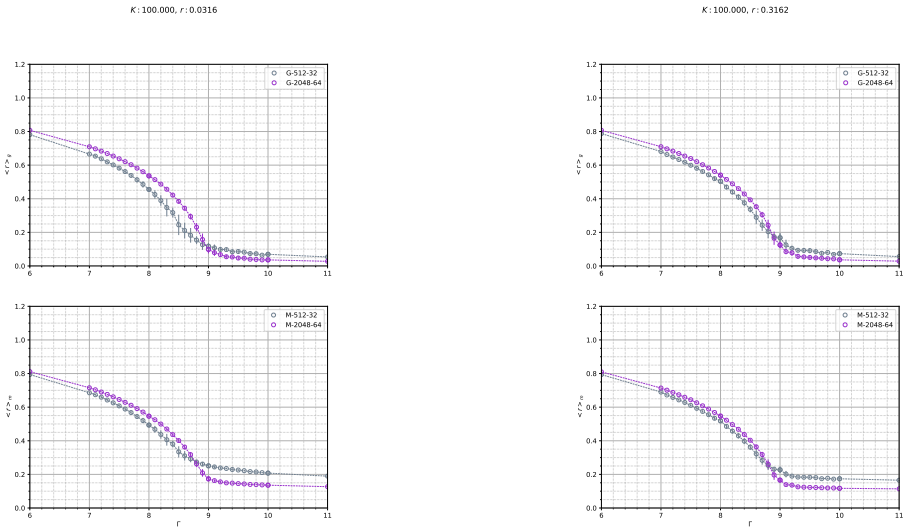

(d) $r = 0.0316$ (e) $r = 0.3162$

Figure 12: Order parameter curves - Kuramoto with external noise. Upper plot is global and lower plot is modular. System sizes are $N = 2048, n = 64$ and $N = 512, n = 32$.

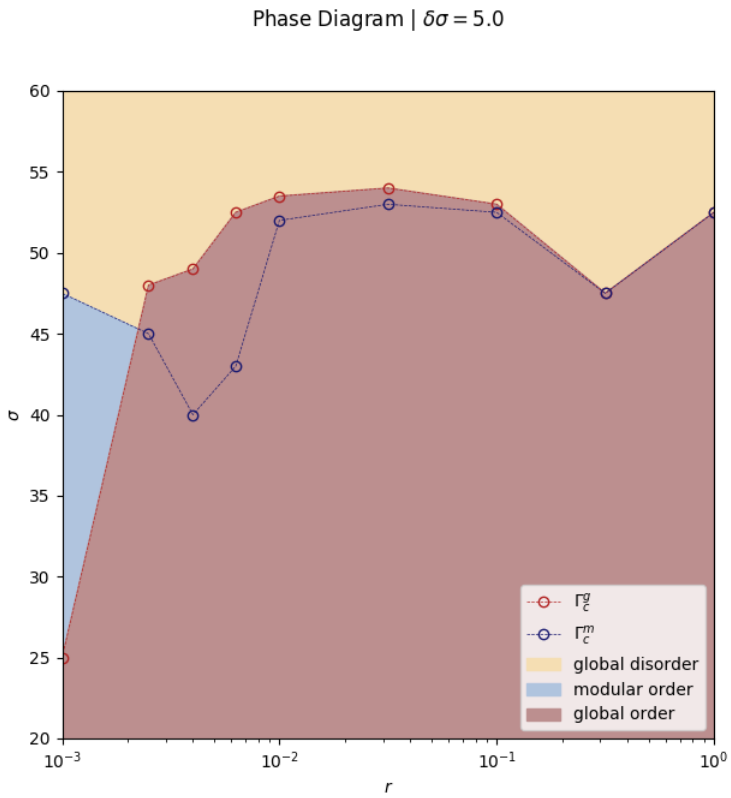

Figure 13: Phase Diagram - Kuramoto model with frequency distribution

3.3 Kuramoto - Frequency distribution

We sample the intrinsic frequencies from a normal distribution, and see how the synchrony varies with variance of the distribution. We observe that for high modularity, we see a modular phase. The phase diagram is given in Fig. 13, constructed by using the intersection of order parameter curves for two system sizes : $512 - 32$, and $2048 - 64$.

3.4 Bimodular network

The network consists of two fully connected modules, and they are connected by a single edge. The frequency of first module is u and second module is v. u is kept constant while v is varied. We observe that at $\Delta\omega = v - u = 0$, we get total synchrony in the network. However, as $v - u$ is gradually increased, global phase coherence is starts to decrease but frequency synchronization is maintained. At modular level, phase coherence is maintained. There exists a non-zero critical $\delta\omega$ beyond which frequency synchronization is also lost. We observe an oscillating global order parameter (Fig. 14), and the frequency ($\dot{\theta}$) of each module starts to oscillate. The modular synchronization remains intact. To better understand this observation, we approximate the system using a simple model in light of the following observations:

1. From our simulations we know that the modular synchronization always occurs, i.e all the oscillators in the module always have the same phase value.

2. All the oscillator in a module are identical except for the one which connects to the other module.

We replace the identical oscillators in a module with a single oscillator, but with a higher coupling ($K \to K(d-1)$), where d is the degree of the oscillator which maintains the inter modular connection. If we write the Kuramoto equations for full system under the constraint of modular synchronization, we will get the same equations as this new system. We have reduced our network of oscillators to a four-oscillator system (Fig. 15). By redefining the phase variables we can reduce

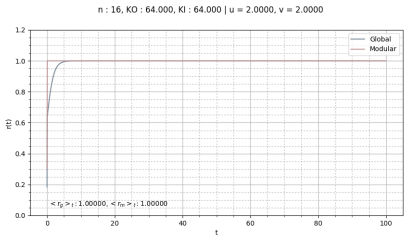

(a) $\Delta\omega = 0$

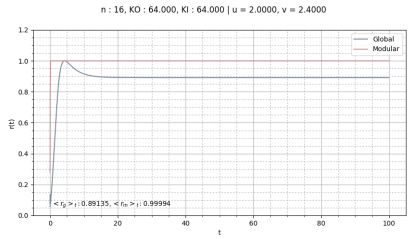

(b) $\Delta\omega = 0.4$

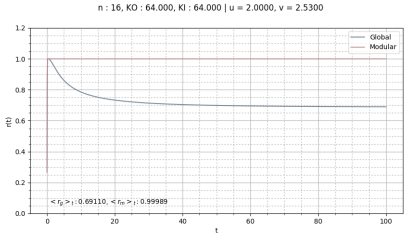

(c) $\Delta\omega = 0.53$

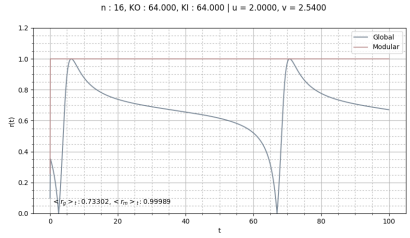

(d) $\Delta\omega = 0.54$

Figure 14: Order parameter - full system. Oscillations are observed in the global parameter after a critical frequency difference (blue). The modular order parameter remains as it is (red).

it to a 3 variable dynamical system which can be studied using linear stability analysis and ODE simulations.

$$x = \theta_2 - \theta_1,\ y = \phi_1 - \theta_1,\ z = \phi_2 - \phi_1 \tag{4}$$

$$\dot{x} = \Delta\omega - \frac{2K}{d}sin(x) + \frac{K(d-1)}{d}[sin(z-x) - sin(y)] \tag{5}$$

$$\dot{y} = -Ksin(y) - \frac{K}{d}sin(x) - \frac{K(d-1)}{d}sin(y) \tag{6}$$

$$\dot{z} = \Delta\omega + Ksin(x-z) - \frac{K}{d}sin(x) - \frac{K(d-1)}{d}sin(y) \tag{7}$$

The results from the linear stability analysis are not yet clear since they differ from the final values obtained from simulation of the ODEs. However, we can make a few conclusions :

1. A non zero $\Delta\omega$ makes the synchronized solution unstable. For zero $\Delta\omega$, the stable fixed point is $(0, 0, 0)$. Non zero $\Delta\omega$ leads to a bifurcation and all the fixed points become saddle.

2. There exists a critical $\Delta\omega$ beyond which linear stability analysis and ODE simulation give different results. Linear stability analysis classifies the fixed point as stable, while ODE simulation shows that it is a saddle point. Fig. 17 and 16.

The saddle point that we see in Fig. 17 is actually the system coming to the same point again and again since the phase space is periodic.

The time series of the variables from the full system and reduced system show similar qualitative behaviour, the critical $\Delta\omega$ is different for them. (Fig. 18)

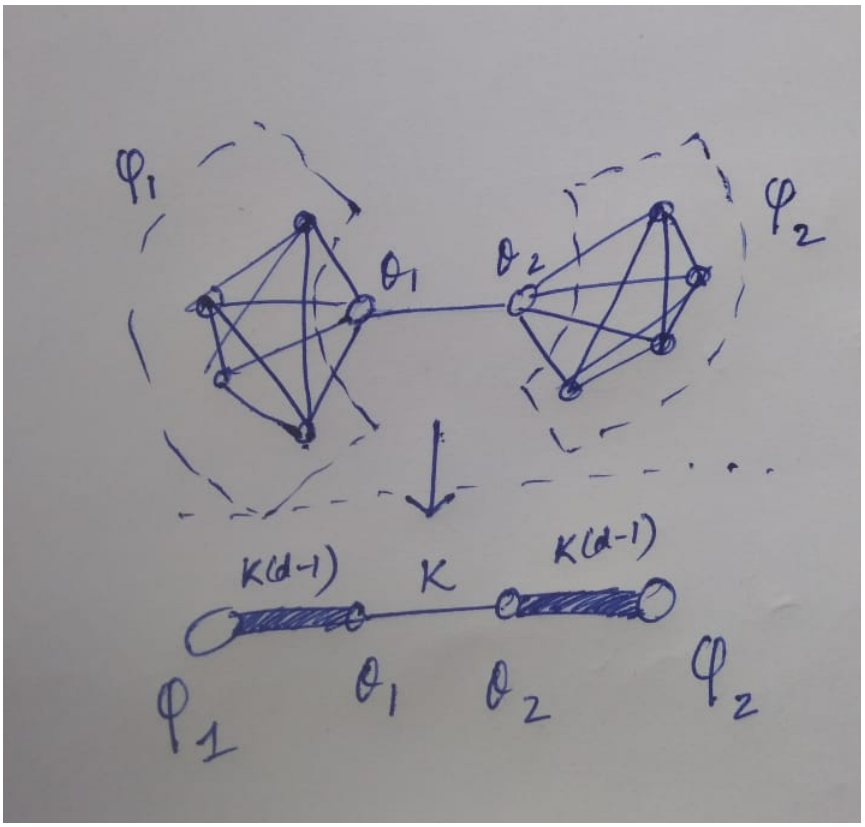

Figure 15: Reduction to four oscillator system.

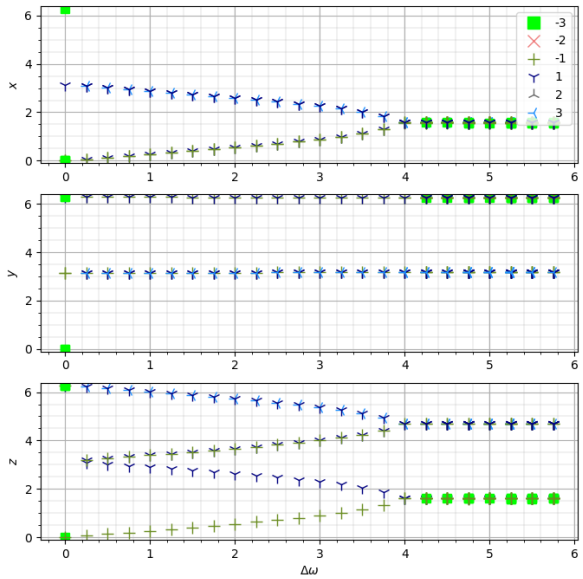

Figure 16: Bifurcation diagram. The legend shows sum of sign(eigenvalues). -3 means all three are negative.

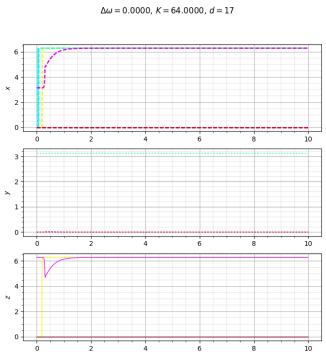

(a) $\Delta\omega = 0$

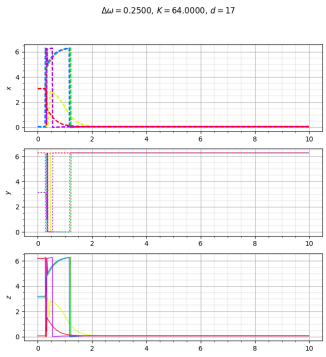

(b) $\Delta\omega = 0.25$

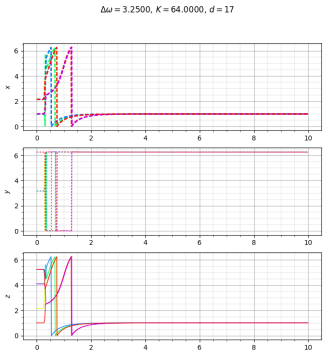

(c) $\Delta\omega = 3.25$

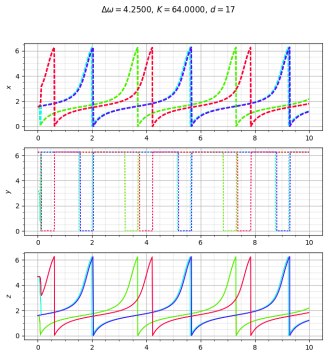

(d) $\Delta\omega = 4.25$

Figure 17: x, y, z time series. Initial conditions are the fixed points obtained from linear stability analysis. We see that beyond $\Delta\omega_c$, we do not see a stable fixed point. It appears to be a saddle point and the system keeps going to the same state (since the phase space is periodic).

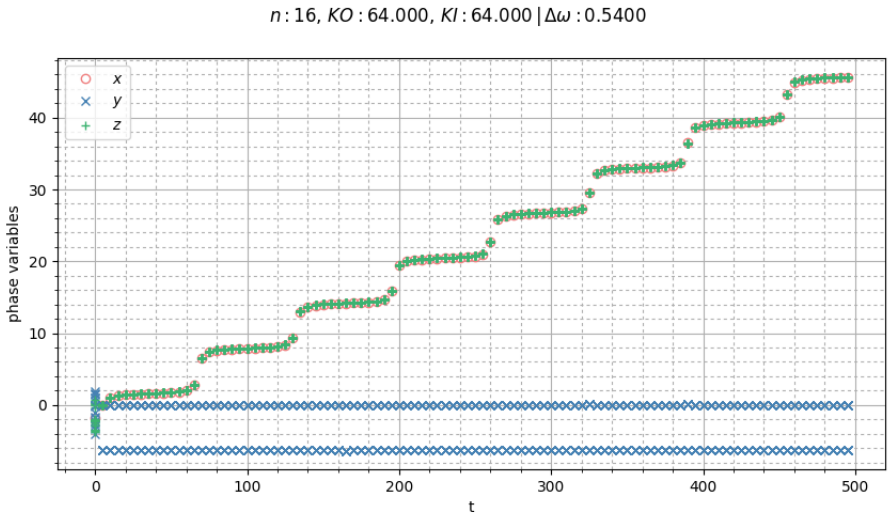

(a) Full system

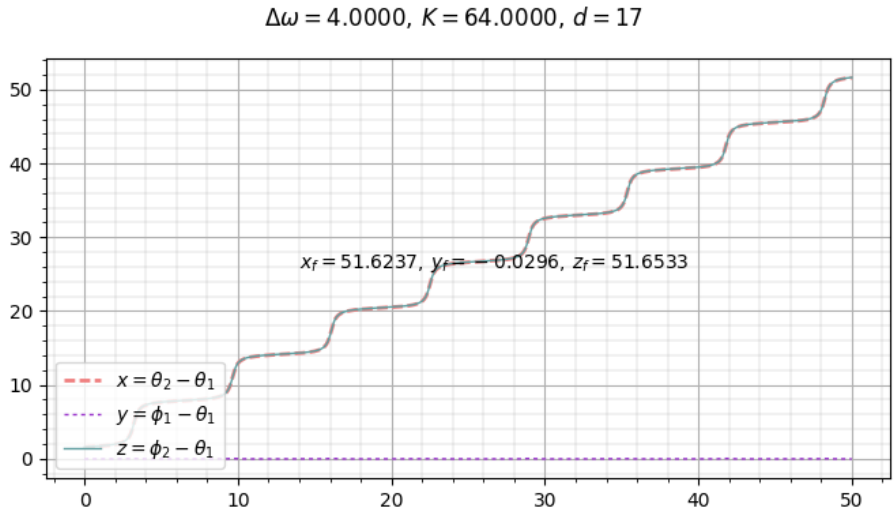

(b) Reduced system

Figure 18: Time series of the phase variables for the full and reduced system show a striking qualitative similarity. Note that here the variables have not been restricted to $[0, 2\pi)$

.

References

[1] Juan A. Acebrón et al. "The Kuramoto model: A simple paradigm for synchronization phenomena". In: *Rev. Mod. Phys.* 77 (1 Apr. 2005), pp. 137–185. DOI: 10.1103/RevModPhys.77.137. URL: https://link.aps.org/doi/10.1103/RevModPhys.77.137.

[2] Kurt Binder and Dieter W Heermann. *Monte Carlo Simulation in Statistical Physics: An Introduction; 5th ed.* Graduate Texts in Physics. Berlin, Heidelberg: Springer, 2010. DOI: 10.1007/978-3-642-03163-2. URL: https://cds.cern.ch/record/1339249.

[3] Subinay Dasgupta, Raj Kumar Pan, and Sitabhra Sinha. "Phase of Ising spins on modular networks analogous to social polarization". In: *Phys. Rev. E* 80 (2 Aug. 2009), p. 025101. DOI: 10.1103/PhysRevE.80.025101. URL: https://link.aps.org/doi/10.1103/PhysRevE.80.025101.

[4] Ulli Wolff. "Collective Monte Carlo Updating for Spin Systems". In: *Phys. Rev. Lett.* 62 (4 Jan. 1989), pp. 361–364. DOI: 10.1103/PhysRevLett.62.361. URL: https://link.aps.org/doi/10.1103/PhysRevLett.62.361.